JOURNAL OF SPACECRAFT AND ROCKETS
Vol. 40, No. 5, September–October 2003

Analysis of Nonstationary Vibroacoustic Flight Data Using a Damage-Potential Basis

S. J. DiMaggio* and B. H. Sako†
The Aerospace Corporation, Los Angeles, California 90009-2957
and
S. Rubin‡
Rubin Engineering Company, Sherman Oaks, California 91403-4708

Traditional maximax analysis of nonstationary flight data for space and launch vehicles can overestimate peak response and does not address the potential for fatigue failure of hardware. A new method, referred to as the damage-based approach, is presented that employs an extended response spectrum analysis and includes amplitude-cycle counts. The outcome is a conservative, stationary test specification that envelops the damage potential of the nonstationary flight environment for both peak response and fatigue, while recognizing uncertainties in damping and the fatigue law. Notable features of the new analysis technique are a quantitative means for addressing fatigue-damage potential in flight and a reduction in the overestimation of peak flight responses. Damage-based analysis of flight data can, therefore, help define more appropriate test specifications from historical data. The new method also provides a more accurate means for assessing the qualification status of components following early missions of a new launch vehicle and may help avoid unnecessary requalification of hardware suggested by an over-conservative maximax analysis of flight data. Potential benefits of the damage-based approach are demonstrated by investigation of a vibration and an acoustic measurement from multiple flights of the Titan 4A launch vehicle.

Nomenclature

A	=	cyclic amplitude, g
$A_{\max}$	=	maximum amplitude, g
$A_{\min}$	=	minimum amplitude for fatigue consideration, g
b	=	fatigue-law exponent
C	=	fatigue-law constant
D	=	fatigue-damage indicator
D_F	=	fatigue-damage indicator for flight
D_T	=	fatigue-damage indicator for test
$D_T^{b=4}$	=	test-damage indicator value for $b = 4$
F	=	fractional damage
f_n	=	oscillator natural frequency, Hz
G	=	acceleration spectral density, g^2/Hz
$k_{n,95,50}$	=	95/50 normal tolerance factor
N	=	number of response cycles
$N_F(S)$	=	number of cycles to cause failure at stress amplitude S
NTL_y	=	normal tolerance limit of y samples
N_0	=	total number of response cycles during test
n	=	number of data samples
$P(A>)$	=	probability that an amplitude exceeds A
$p(A)$	=	probability density for an amplitude A
Q	=	modal quality factor
S	=	stress cycle amplitude resulting from motion amplitude A, Pa
s_y	=	sample standard deviation
$T(A>)$	=	total duration of response cycles which equal or exceed the amplitude A, s
$T(S)$	=	total duration of response cycles with stress amplitude S, s
T_0	=	test duration, s
y	=	samples
$\bar{y}$	=	sample mean
α	=	proportionality factor relating stress to acceleration
σ	=	standard deviation of response

Subscripts

b	=	fatigue-law exponent
F	=	flight-related value
i	=	ith bin
T	=	test-related value
1	=	spectrum controlled by maximum amplitude
2	=	spectrum controlled by amplitudes less than the maximum
4	=	spectrum corresponding to fatigue-law exponent of 4
8	=	spectrum corresponding to fatigue-law exponent of 8
12	=	spectrum corresponding to fatigue-law exponent of 12

Received 9 September 2002; revision received 13 January 2003; accepted for publication 5 February 2003; presented as Paper 2003-1973 at the AIAA Dynamics Specialists Conference, Norfolk, VA, 7–10 April 2003.

*Project Leader, Environmental Test and Ordnance Department, P.O. Box 92957-M4/910. Member AIAA.
†Senior Engineering Specialist, Structural Dynamics Department, P.O. Box 92957-M4/911. Member AIAA.
‡Consultant, 3531 Alana Drive. Associate Fellow AIAA.

Introduction

QUALIFICATION, acceptance, and protoflight vibroacoustic test requirements for space and launch vehicle hardware are typically defined and verified by using flight data. Whereas the tests are normally conducted by using stationary random excitation, equipment is exposed to nonstationary environments in flight. To deal conservatively with the nonstationarity, the maximax spectrum has traditionally been used. It has been observed, from a damage-potential standpoint, that the maximax approach can yield overly conservative values of test spectra when brief periods of strong, narrow-band oscillation occur in flight. Furthermore, the traditional maximax method is not capable of determining the potential for fatigue-damage accumulation in flight, or providing a comparison of this potential with what the equipment was subjected to during its qualification testing.

Traditional maximax processing of flight data determines an upper bound of the power spectral density for a sequence of short time intervals (piecewise stationary analysis). The resulting spectrum

depends on processing parameters such as the averaging time and the frequency resolution (bandwidth) of the analysis. The problems associated with using the maximax data analysis procedure to estimate peak responses in nonstationary space and launch vehicle environments are well known, and processing-parameter optimization to minimize errors resulting from nonstationarity in the flight data has been documented.[1–5] Unfortunately, the optimum choice of parameters discussed in the earlier work is measurement dependent and is not related to physical properties of the hardware, such as modal quality factor, that are easy for a vibroacoustics engineer to understand. Guidelines for development of acceptance and qualification test criteria by using the maximax spectral approach may be found in Refs. 6–11.

An alternate method, referred to as the damage-based approach, is described herein and determines random test requirements that envelop the damage potential of the nonstationary flight environment. The damage-based method applies the flight data as a forcing function to a series of single-degree-of-freedom (SDOF) oscillators that represent vibration modes of hardware experiencing the environment. No Fourier analysis is involved, and so errors resulting from piecewise stationary analysis of nonstationary data are avoided. The method was developed by Rubin,[12] and a computer implementation was developed by Sako at The Aerospace Corporation. The approach taken ensures that the peak responses and the fatigue-damage potential experienced by the equipment (represented by the SDOF oscillators) during flight are enveloped by the corresponding responses expected during an equivalent stationary test. The fundamental approach used herein makes use of many of the concepts discussed by Lalanne.[13,14] Miskel,[15] under the guidance of Rubin, later addressed the optimization of the test spectrum and the time duration that minimizes the effect of uncertainty in the fatigue-law exponent.

Although the damage-based analysis process is more complicated than the maximax approach, the same resulting form of test specification is retained. In comparison to the traditional maximax approach, the significant advantages of the damage-based approach are believed to be the following: First, damage potential due to fatigue accumulation, as well as to peak response, is evaluated in a well-accepted, quantitative manner by using an extended response spectrum approach. Second, in comparison to the maximax approach, the damage-based method reduces the overestimation of spectral peak values caused by brief periods of strong oscillation in the flight data. Third, processing errors resulting from the assumption of stationarity, necessary for maximax processing, are eliminated. Finally, fatigue-damage contributions from different phases of flight, such as liftoff and transonic events, are easily combined because the damage-indicator values described herein are commutative.

A primary motive for development of the damage-based analysis approach is to avoid a costly overreaction to maximax results from early missions of a new launch vehicle that indicate inadequate qualification of equipment. This paper demonstrates that significant reduction in levels can be achieved by using the damage-based data processing techniques described herein. It is suggested that such reduction may form the basis for avoiding a requalification or vibration reduction process that may appear necessary because of maximax processing of flight data. The damage-based analysis tool is also expected to be incorporated into the Vibroacoustic Intelligent System for Predicting Environments, Reliability, and Specifications.[16]

The objectives of this document are to introduce the damage-based approach and to demonstrate the potential advantages of the technique by investigation of two statistically meaningful sets of launch vehicle flight data. An evaluation of the new approach is based herein on Titan 4A launch vehicle flight data obtained for a vibration measurement acquired on 12 different missions and an acoustic measurement obtained on 15 different missions. To meet the objectives, this paper is organized as follows. First, the traditional maximax approach is reviewed. Then, the damage-based approach proposed in the present study is described in detail. Last, a comparison of the spectra obtained from the two approaches is presented for environments observed on the Titan 4A launch vehicle.

Traditional Maximax Approach

Prediction and verification of the maximum-predicted random environments for space and launch vehicles depends on the analysis of flight data acquired during a series of events throughout the ascent stage of a rocket. These events are labeled in Fig. 1 on a time history of vibration acquired at 5000 samples per second on the instrumentation truss of the Titan 4A launch vehicle. Note the obvious nonstationary character of the data that contain time-varying events including liftoff, transonic flight, and aerodynamic pressure oscillations during passage through maximum dynamic pressure. The instrumentation truss on the Titan 4A launch vehicle is located in compartment 2A, which is just aft of the payload fairing boattail as shown in Fig. 2. Several narrow-band oscillations occurred with a much greater degree of nonstationarity than is inferred from the envelope variation of the broadband vibration shown in Fig. 1. An example of the nonstationary character of narrow-band flight data is shown in Fig. 3 for the time variation of the 1-s-average rms value in a $\frac{1}{6}$th-octave band centered at 223.6 Hz. A narrow-band spectral

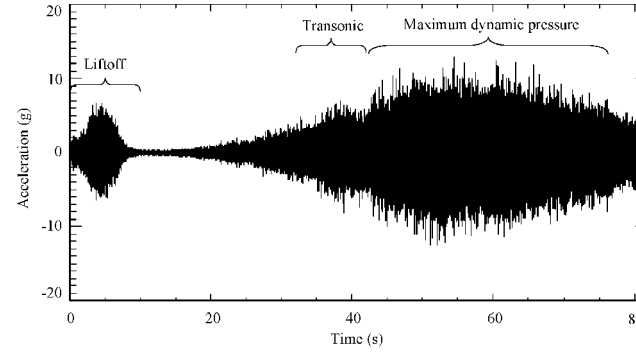

Fig. 1 Typical vibration time history response acquired during the ascent stage of Titan 4A launch vehicle mission K-22.

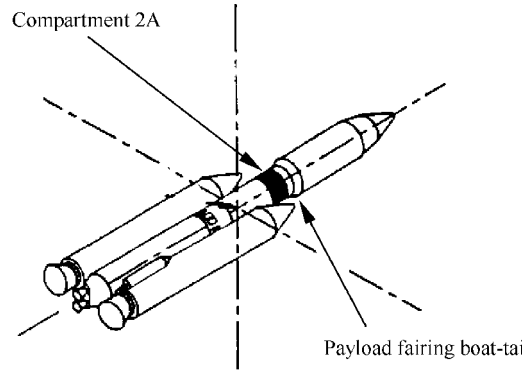

Fig. 2 Titan 4A launch vehicle with compartment 2A identified by the gray shaded region just aft of the payload fairing boattail.

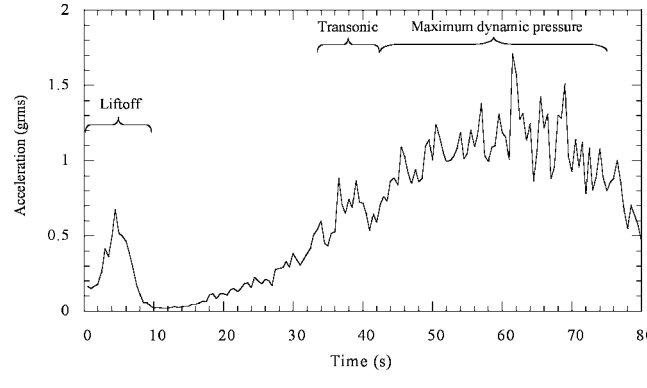

Fig. 3 RMS acceleration vs time in a one-sixth-octave band centered at 223.6 Hz acquired using a 1-s averaging time for the vibration measurement shown in Fig. 1.

peak from analysis of flight data serves to establish a plateau region in a test spectrum. As exemplified in Fig. 3, the maximax value can be the value in only one averaging-time period that is well above the value at other times. The degree of conservatism in the peak value obtained by using the maximax approach can, therefore, be large when only a brief period of strong oscillation occurs during the flight.

Power spectra that have historically been established in fractional-octave bands by using either analog instruments or filters implemented on digital computers are now commonly estimated by using Fourier transform-based digital signal processing techniques.[17,18] During each time slice, a constant-bandwidth power spectral density (PSD) is computed and then averaged within fractional-octave bands. The overall maximax PSD is then the envelope of the fractional-octave-band PSDs in all of the time slices. The maximax spectra presented herein use the traditional processing for Titan flight data: 1-s time slices, with 50% overlap, to determine a one-sixth-octave-band vibration spectrum or a one-third-octave-band acoustic spectrum.[8–11]

Damage-Based Approach

Unlike traditional methods used for development of test criteria, the damage-based approach creates a stationary test that attempts to envelop the resonant responses, rather than the input, experienced by the hardware in flight. Potential resonant responses are determined by using an extended response spectrum approach. The flight data are applied as input to a series of SDOF oscillators described by their natural frequencies f_n and modal quality factors Q. Because resonant characteristics of the hardware are often unknown, the approach taken is to assume that resonances exist over the entire frequency region of interest (10–2000 Hz), and a range of Q is used to span the uncertainty in damping. To avoid significant smoothing of results from strong narrow-band responses, the results presented are based on SDOF oscillators located with a 1/12-octave spacing of their natural frequencies. The 1/12-octave spacing contrasts with the smoothing inherent in traditional processing wherein spectra are averaged into $\frac{1}{6}$-octave bands for vibration and $\frac{1}{3}$-octave bands for acoustics.

A detailed description of the damage-based approach is presented in the following five subsections of this paper. First, some fundamental concepts related to stationary random vibration are reviewed. Second, a procedure for plotting and evaluating nonstationary flight data is outlined. Then, a quantitative method for assessment of fatigue-damage potential in flight is introduced in the context of a flight-damage indicator. Finally, a test-damage indicator is defined and a method for determining a fatigue-equivalent stationary test that envelops the damage potential experienced in flight is described.

Stationary Random Vibration

The distribution of peak values in a narrowband random vibration is the Rayleigh distribution. Applied to the response of a lightly damped SDOF oscillator excited by a zero-mean, stationary, Gaussian, white noise input, the probability density function for an amplitude A is

$$p(A) = (A/\sigma^2)\exp(-A^2/2\sigma^2), \qquad A \geq 0 \quad (1)$$

For this zero-mean process, the standard deviation is equal to the rms value. Integrating Eq. (1) from some amplitude A to infinity gives the probability that cycles have an amplitude greater than A, that is,

$$P(A>) = \exp(-A^2/2\sigma^2) \quad (2)$$

If one considers a stationary test of duration T_0, the total time $T(A>)$, or cumulative duration, spent during which response cycles with amplitudes exceeding A occur is

$$T(A>) = T_0 P(A>) = T_0 \exp(-A^2/2\sigma^2) \quad (3)$$

Taking the natural logarithm of both sides of Eq. (3) yields

$$\ln[T(A>)] = \ln(T_0) - (A^2/2\sigma^2) \quad (4)$$

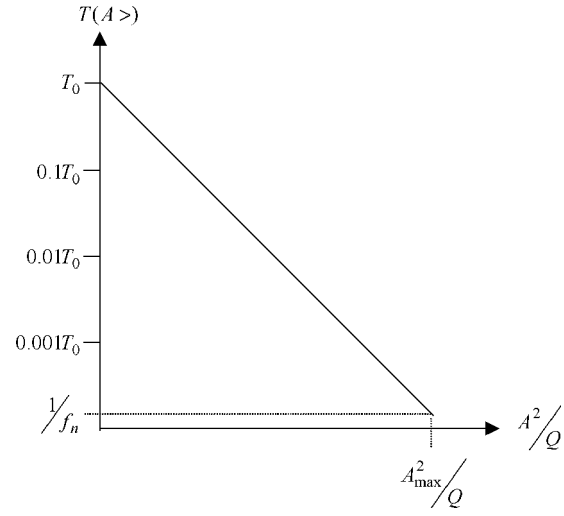

Fig. 4 Plot form yielding a straight line for the logarithm of the time that response cycles exceed A^2/Q.

For SDOF acceleration response to a broadband Gaussian excitation with acceleration spectral density G, the variance, or mean-square response, is approximated by the well-known result for the case of small damping, that is,

$$\sigma^2 \cong (\pi/2)Gf_nQ \quad (5)$$

Substituting Eq. (5) into Eq. (4) yields

$$\ln[T_0/T(A>)] = (1/\pi Gf_n)(A^2/Q) \quad (6)$$

For a particular value of f_n, the function in Eq. (6) appears as a straight line on a plot of log $T(A>)$ vs linear A^2/Q, as shown in Fig. 4. In Fig. 4, $A_{\max}$ is the expected maximum amplitude occurring at the exceedence duration of one period.

Flight Data Evaluation

The first step in a damage-based analysis requires plotting SDOF oscillator responses to nonstationary flight data in the format shown in Fig. 4. The plot format of Fig. 4 provides a powerful visual aid to assess the degree to which the peak responses during flight at a particular natural frequency are Rayleigh-like and, thus, the reasonableness of specifying a stationary random test. Response is calculated for several values of Q to encompass damping uncertainty. Prescribing a test based on an enveloping Rayleigh line guarantees that the damage potential of the test, for a resonance at that frequency, envelops the damage potential of flight over the range of damping uncertainty.

The procedure used for plotting the flight data in the same manner as shown in Fig. 4 is outlined by nine points as follows: First, on a logarithmic scale, set up a series of bins for accumulating cyclic values of A^2/Q. In the following terminology, low bins correspond to small values of A^2/Q and high bins correspond to large values of A^2/Q. Second, determine the response for selected values of f_n and Q. For flight acceleration data, the absolute acceleration response of a unit mass to a base acceleration input is calculated. For the flight pressure data, the acceleration response of a unit mass to a force equal to the pressure acting over a unit area is calculated. Find the amplitude A for each cycle of response and add one count to the A^2/Q bin into which it falls, as well as adding one count in each lower bin. After all cycles are placed into the appropriate bins, the count n_i in the ith bin is the number of cycles having an A_i^2/Q value falling in that bin added to all of the cycles falling in higher bins. Because each cycle has a period $1/f_n$, the number of cycles in the ith bin is also used to determine the total time that responses occur with an amplitude greater than or equal to A_i, namely, $T(A_i>) = n_i/f_n$. For a complete description of the cycle and amplitude identification procedure used herein, see Refs. 12 and 15. Third, plot the logarithm of the cumulative duration $T(A>)$ vs

the linear value of A^2/Q. Fourth, repeat steps two and three for other values of Q and the same f_n. An example plot of results appears in Fig. 5, which shows the results of analysis for the Titan 4A mission K-3, vibration measurement 9509 flight data at a natural frequency of 14.14 Hz and Q values of 10, 25, and 50. Note that 9509 is a numerical identifier for a transducer used to acquire the vibration measurement on the instrumentation truss of the Titan 4A launch vehicle. The data are plotted in the format shown in Fig. 4. Based on a 60-s test, a line to the observed maximum response amplitude at a Q of 25 envelops all of the data and corresponds to an input acceleration spectral density designated G_1. Fifth, for each value of f_n, assess the reasonableness of a stationary random test in terms of the degree of similarity of the curves for the several values of Q to the straight line expected for the Rayleigh distribution (Figs. 4 and 5). Sixth, if a stationary random test appears to be reasonable, review the plots to select a test duration T_0, keeping in mind that the Rayleigh line starts at T_0 and $A^2/Q = 0$. A line from T_0 to the maximum value $A^2_{\max}/Q$ at the duration of one period, or $1/f_n$, should reasonably envelop the data for all Q values, except for low values of A^2/Q as discussed in point 8 subsequently. Seventh, by using Eq. (6) and Fig. 4, the spectral density corresponding to the line from T_0 to $A^2_{\max}/Q$ is

$$G_1 = \frac{\left(A^2_{\max}/Q\right)}{\pi f_n \ell n(f_n T_0)} \tag{7}$$

Eighth, when the flight results bulge above the line from T_0 to $A^2_{\max}/Q$, a second line is drawn from T_0 to just encompass all of the data. This second straight line leads to a higher value, designated as G_2. An example appears in Fig. 6, which shows the results of analysis for the Titan 4A mission K-3, vibration measurement

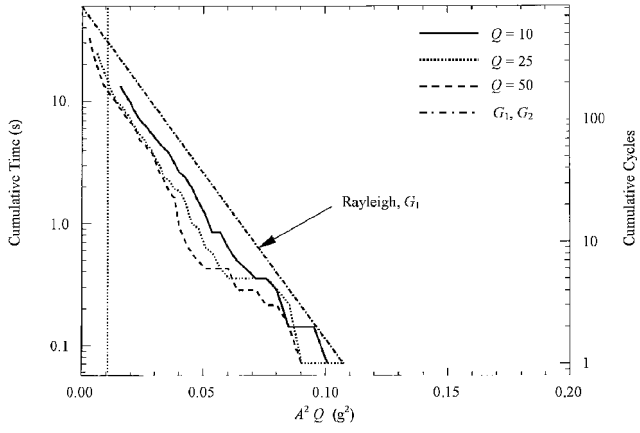

Fig. 5 Results of analysis on Titan 4A mission K-3: vibration measurement 9509 flight data at a natural frequency of 14.14 Hz.

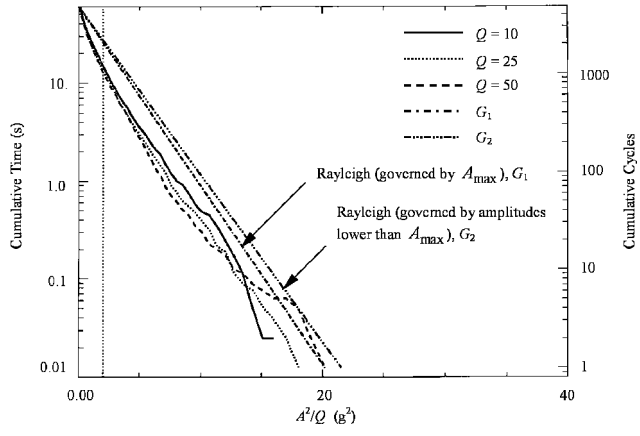

Fig. 6 Results of analysis on Titan 4A mission K-3: vibration measurement 9509 flight data at a natural frequency of 80.00 Hz.

9509 flight data at a natural frequency of 80.00 Hz and Q values of 10, 25, and 50. Again, the data are plotted in the format shown in Fig. 4. Figure 6 is an example where the line to $A_{\max}$, the maximum observed amplitude, does not envelop all of the data. The line that does envelop all of the data leads to a G_2 value that is greater than the G_1 value for the line to $A_{\max}$. Bulges in the flight data that occur below the dotted-line limit on A^2/Q (shown in Figs. 5 and 6) are not considered in the determination of G_2. For the analysis presented here, this lower limit was set to 1/10th of the value of $A^2_{\max}$ (a little over $A_{\max}/3$) with the objective of avoiding amplitudes likely to be below the fatigue endurance limit. For aluminum alloys, Steinberg[19] states that the endurance stress is typically one-third of the ultimate tensile stress. Use of one-third of the measured $A_{\max}$ to define the dotted-line limit, rather than the acceleration corresponding to ultimate conditions, is, therefore, a conservative way to approximate the limit below which response cycles are not significant for the determination of G_2. A different value for the endurance limit can be chosen based on the knowledge of relevent fatigue characteristics. Ninth, once G_1 and G_2 are determined for all frequencies, a stationary random test spectrum is defined to envelop these values, with T_0 as the test duration.

The nine-point procedure just described ensures that equipment being tested will experience a given number of cycles and a corresponding set of amplitudes that are greater than or equal to the amplitudes and cycles experienced during the nonstationary flight environment. Local peaks in G_1 and G_2 should be extended over a reasonable frequency band by the specification enveloping process and a typical guideline is to maintain a peak value at least over a $\pm 10\%$ range of the center frequency of the peak.

Fatigue Assessment

In addition to the potential for equipment damage because of peak stresses, the potential for high-cycle-fatigue damage should also be considered. An alternate assessment (as opposed to G_2) of fatigue-damage potential is based upon two fundamental assumptions. The first is that the fractional damage F obeys the Miner–Palmgren hypothesis given by

$$F = \sum_i \frac{N(S_i)}{N_F(S_i)} \tag{8}$$

where $N(S_i)$ is the number of stress cycles with amplitude S_i and $N_F(S_i)$ is the number of cycles at S_i necessary to cause failure. Failure is predicted when F reaches a value of unity. The second assumption is that the number of cycles necessary to cause failure obeys the following idealized S–N law for stress amplitudes above the endurance limit:

$$S_i^b N_F(S_i) = C \tag{9}$$

where b is the fatigue-law exponent and C is a constant. The fractional damage is then expressed as

$$F = \frac{1}{C} \sum_i S_i^b N(S_i) \tag{10}$$

The duration of stress response cycles of S_i having the frequency f_n is

$$T(S_i) = N(S_i)/f_n \tag{11}$$

Including the proportionality of stress to the response motion, or $S = \alpha A$, the fractional-damage expression for response motion of an SDOF system is

$$F = \frac{\alpha^b f_n}{C} \sum_i A_i^b T(A_i) \tag{12}$$

For the relation of damage potential between a flight environment and a test, it is only necessary to compare the values of the terms

within the summation sign in Eq. (12). The value of this summation is designated as a fatigue-damage indicator D given by

$$D = \sum_i A_i^b T(A_i) \tag{13}$$

Note that the value of this fatigue-damage indicator is proportional to the actual fractional damage F, but the constant of proportionality $\alpha^b f_n/C$ is unknown. Determination of the constant of proportionality is unnecessary if it does not change from flight to test, as is assumed herein. Cases where the material properties are different during flight and ground testing are not covered in this document and require an extension to the current approach.

Flight-Damage Indicator

The processing of flight data places response amplitudes into bins based on A_i^2/Q and determines the cumulative time spent by amplitudes within and above each bin, or $T(A_i>)$. In these terms, the flight-damage indicator is written as the following form of Eq. (13):

$$D_F = Q^{b/2} \sum_i \left(\frac{A_i^2}{Q}\right)^{b/2} T(A_i) \tag{14}$$

where $T(A_i)$ is the time spent in the ith bin, calculated by

$$T(A_i) = T(A_i>) - T(A_{i+1}>) \tag{15}$$

Test-Damage Potential

It is now desired to develop the stationary Gaussian test inputs G_b that will theoretically produce test fatigue-damage indicator values D_T that are equivalent to the corresponding D_F for a fatigue exponent of b. Using Eq. (1), the fractional time spent at an amplitude A, for a test of duration T_0, is

$$T(A)/T_0 = p(A) = (A/\sigma^2)\exp(-A^2/2\sigma^2) \tag{16}$$

When a continuous form of Eq. (13) is used, the test-damage indicator value is defined as

$$D_T = \int A^b T(A)\,\mathrm{d}A \tag{17}$$

Inserting $T(A)$ from Eq. (16) into Eq. (17), making A^2 the variable of integration, and introducing limits on the integration yields

$$D_T = \frac{T_0}{2\sigma^2} \int_{A_{\min}^2}^{A_{\max}^2} (A^2)^{b/2} \exp\left(\frac{-A^2}{2\sigma^2}\right) \mathrm{d}(A^2) \tag{18}$$

Equation (18) is evaluated by repeated integration by parts for fatigue exponents of 4, 8, and 12, as detailed in Ref. 12. The upper limit of integration $A_{\max}^2$ is chosen such that only one higher response cycle is expected, on average, during the equivalent stationary test and is expressed mathematically by

$$N_0 P(A_{\max}>) = 1 \tag{19}$$

where

$$N_0 = f_n T_0 \tag{20}$$

is the total number of response cycles in the test. Equations (2), (19), and (20) yield

$$A_{\max}^2 = 2\sigma^2 \ln(f_n T_0) \tag{21}$$

The lower limit of integration in Eq. (18), chosen based on the endurance ratio of the material, can be expressed as a fraction of $A_{\max}$. Recall that a lower limit on amplitude, for the same purpose, was discussed earlier in connection with enveloping response-amplitude counts from flight data and that $0.1(A_{\max}^2)$ was chosen. For application to a stationary test, a lower bound of $0.1(A_{\max}^2)$ has a negligible effect, and so it is set to zero. By using the normalized amplitude

$$\bar{A}_{\max}^2 = A_{\max}^2/\sigma^2 = 2\ln(f_n T_0) \tag{22}$$

the closed-form expression for the test-damage indicator value for $b=4$ is

$$D_T^{b=4} = T_0\sigma^4\left[8 - \exp\left(-\bar{A}_{\max}^2/2\right)\left(\bar{A}_{\max}^4 + 4\bar{A}_{\max}^2 + 8\right)\right] \tag{23}$$

Note that Eqs. (22) and (23) are functions of the test duration, the natural frequency of the oscillator, and the unknown response variance. When the test-damage indicator $D_T^{b=4}$ is equated with the corresponding flight-damage indicator, determined by using Eq. (14) with $b=4$, the response variance σ^2 that will produce a test with an equivalent flight-damage indicator is determined by using Eq. (23). Closed-form solutions for $b=8$ and 12 are also functions of the same variables and are defined in Ref. 15. Finally, stationary Gaussian test inputs G_4, G_8, and G_{12}, corresponding to fatigue exponents of 4, 8, and 12, respectively, are determined from the response variances by using Eq. (5). Note that this procedure of equating test- and flight-damage indicator values is performed at each natural frequency and for each value of Q.

In the following examples, the damage-based test spectrum G_{test} is the maximum value obtained from G_1, G_2, G_4, G_8, and G_{12} for each of the quality factors $Q=10$, 25, and 50. Conservatism is maintained, therefore, through the degree of uncertainty in damping and the fatigue exponent.

Titan 4A Launch Vehicle Environments

This section provides a comparison of Titan 4A launch vehicle spectra obtained by using the damage-based approach and the maximax approach. For the damage-based approach, vibration spectra are produced at 1/12-octave center frequencies and are compared to maximax spectra computed in $\frac{1}{6}$-octave bands. For acoustic data, the damage-based spectra are computed at 1/12-octave center frequencies and then converted and compared to $\frac{1}{3}$-octave maximax sound pressure levels (SPLs). The following two subsections will present results from a set of vibration and acoustic measurements, respectively.

Vibration Results

Vibration data were acquired on the instrumentation truss in compartment 2A of the Titan 4A launch vehicle, shown in Fig. 2, on 12 different flights. This measurement, referred to herein as 9509, presents a rare opportunity, for aerospace launch vehicles, to investigate the response at the same location on repeated flights. In the present study, a comparison of results is based on the 95/50 normal tolerance limit of the sample data, the overall rms level from the 95/50 results, and the differences in the spectral values at peaks in two frequency ranges of special interest.

At each frequency, the 95/50 normal tolerance limit (NTL) for the 12 data samples is defined:

$$\mathrm{NTL}_y(f) = \bar{y}(f) + k_{n,95,50}\, s_y(f) \tag{24}$$

where $\bar{y}(f)$ and $s_y(f)$ are the average and standard deviation of the samples y and $k_{n,95,50} = 1.69$ for $n=12$ flights. Note that the NTL applies only to normally distributed random variables and is used extensively for developing conservative limits for structural response in the aerospace industry. The value of $\mathrm{NTL}_y(f)$ in Eq. (24) is that value of y that will exceed at least 95% of all possible values of y, with a confidence of 50%. It is typical[6] in the aerospace industry to assume that the vibration spectral-density values have a lognormal distribution with a standard deviation bounded by 3 dB, which is the value typically used for $s_y(f)$ in Eq. (24). In the present study, the actual sample mean and standard deviation of the data at each frequency are used for the 95/50 comparison of the maximax to the damage-based results shown in Fig. 7.

In Fig. 7, notice the overestimation of 95/50 spectral peaks obtained by using the maximax approach, relative to the peaks determined using the damage-based method, in the 31.5–63- and 160–250-Hz frequency ranges by 5.9 and 2.9 dB, respectively. These frequency ranges are of primary interest because of the known location of two structural modes in the 31.5–63-Hz region and another resonance that occurs between 160 and 250 Hz. Also, note that

Table 1 Spectral peak values obtained using maximax approach (decibels)

Frequency range, Hz	Mission												Minimum	Mean	Maximum
	K-3	K-8	K-10	K-11	K-14	K-15	K-16	K-17	K-19	K-21	K-22	K-23			
31.5–63	−7.55	−7.74	−5.52	−7.68	−8.66	−5.30	−11.12	−8.43	−9.67	−7.73	−9.11	−10.01	−11.12	−8.21	−5.30
160–250	−6.48	−8.26	−8.01	−7.36	−8.95	−6.21	−9.04	−9.06	−8.10	−8.33	−9.29	−12.40	−12.40	−8.46	−6.21

Table 2 Spectral peak values obtained using damage-based approach (decibels)

Frequency range, Hz	Mission												Minimum	Mean	Maximum
	K-3	K-8	K-10	K-11	K-14	K-15	K-16	K-17	K-19	K-21	K-22	K-23			
31.5–63	−10.17	−9.95	−13.23	−12.22	−12.37	−12.24	−14.05	−15.20	−16.97	−12.86	−12.19	−13.38	−16.97	−12.90	−9.95
160–250	−8.60	−11.97	−10.87	−9.57	−11.37	−9.34	−10.85	−12.32	−9.12	−10.87	−11.99	−14.68	−14.68	−10.96	−8.60

Table 3 Differences between damage-based and maximax spectral peaks (decibels)

Frequency range, Hz	Mission												Minimum	Mean	Maximum
	K-3	K-8	K-10	K-11	K-14	K-15	K-16	K-17	K-19	K-21	K-22	K-23			
31.5–63	2.62	2.21	7.71	4.54	3.72	6.94	2.93	6.78	7.31	5.14	3.08	3.37	2.21	4.69	7.71
160–250	2.12	3.71	2.86	2.20	2.41	3.12	1.81	3.26	1.02	2.55	2.70	2.28	1.02	2.50	3.71

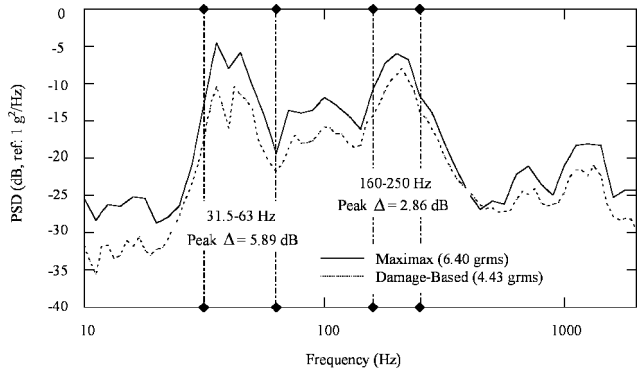

Fig. 7 Comparison of 95/50 levels for vibration measurement 9509 acquired on the instrumentation truss in compartment 2A for 12 flights of the Titan 4A launch vehicle.

the overall rms level (from 10 to 2000 Hz) obtained by using the damage-based approach (4.43 *g* rms) is more than 30% lower than that obtained by using the maximax approach (6.40 *g* rms). If these flight data were used to develop test specifications for equipment on a new launch vehicle, as is often done in the aerospace industry, reduced qualification levels for the new hardware might be warranted by the more realistic interpretation of the historical spectra obtained by using the damage-based approach. Whereas conservatism in generating test specifications is desirable, an excessive amount can cause undesirable qualification test methods, such as band splitting, to be employed because of limitations in shaker capability. Note that band splitting requires splitting the qualification spectrum into several frequency bands and subjecting the qualification unit to random vibration in each band separately. This undesirable test method, therefore, does not account for the potential of a multimode failure mechanism, in which resonant response of modes in different test bands may occur simultaneously in flight. Although the low rms level for measurement 9509 would not necessitate band splitting, many of the criteria set for newer rockets have dictated that this test procedure be used. The savings of over 30% in the overall rms level for measurement 9509 suggests that using the damage-based approach for interpreting historical flight data may give an analyst the confidence necessary to set reduced, yet still conservative, specification levels that may lead to less band splitting during qualification testing.

In addition to the 95/50 results, Tables 1 and 2 present the spectral peak values in the two frequency ranges of primary interest, along with the minimum, mean, and maximum values for all available missions. Table 3 demonstrates the differences in spectral peak values obtained by subtraction of the damage-based results from the maximax results. Note that for certain missions, the damage-based approach yields spectral peak values as much as 7.7 and 3.7 dB lower for the 31.5–63- and 160–250-Hz frequency ranges, respectively. Table 3 also indicates that by using the damage-based approach, significantly lower spectral peak levels are obtained on average, and, in fact, the smallest reductions for any mission are 2.2 and 1.0 dB for the 31.5–63- and 160–250-Hz frequency ranges, respectively.

Test specifications are usually defined by using straight-line segments in log–log plots of spectral density. Consider that historical data had been used, before the initial Titan 4A flight, to generate a qualification level defined by a straight line at −8 dB across the 10–2000-Hz frequency range of interest. Tables 1 and 2 indicate that this qualification level would have been exceeded on many missions (especially the early ones) if traditional maximax processing was used, but would not have been exceeded even once if the damage-based approach was employed. In other words, if the qualification levels were indeed as considered (in reality they were not), a costly requalification process might have been mandatory if maximax analysis of the flight data had been used, whereas if the damage-based approach had been applied, no retesting of the hardware would have been considered. Although the situation discussed here is hypothetical, the example does demonstrate the significant potential benefit of using the damage-based approach for flight-data analysis on a new launch vehicle.

Acoustic Results

Data acquired from a flush-mounted microphone, referred to herein as 9675, were acquired on the exterior of compartment 2A of the Titan 4A launch vehicle during 15 missions. Figure 8 presents a comparison of the 95/50 normal tolerance limits for the free-field SPL calculated by using both the maximax method and the damage-based approach. Similar to the vibration results, notice the significantly lower overall SPL obtained from the damage-based method (158.6 dB) as compared to the maximax result (161.2 dB). Also, in the frequency range at and below 200 Hz, the damage-based approach again demonstrates that maximum response can be substantially overestimated; in this case by 3.9 dB, when the traditional maximax method is used.

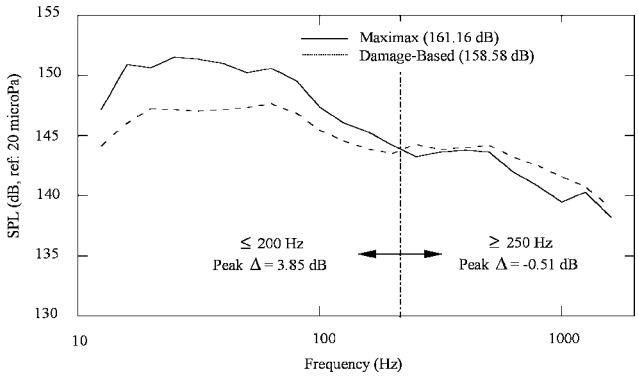

Fig. 8 Comparison of 95/50 levels for acoustic measurement 9675 acquired on the exterior of compartment 2A for 15 flights of the Titan 4A launch vehicle.

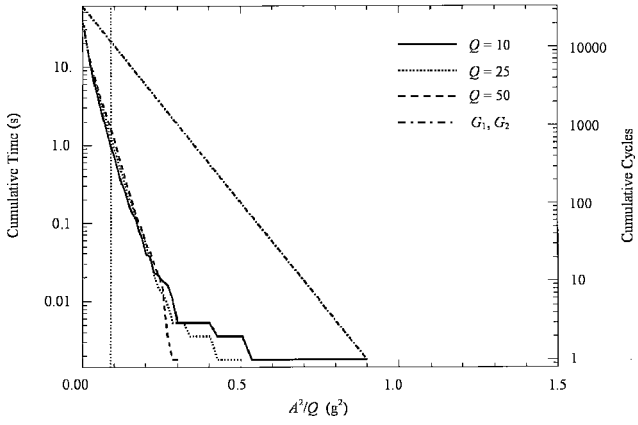

Fig. 9 Results of analysis on Titan 4A mission K-3, acoustic measurement 9675 flight data at a natural frequency of 561.2 Hz.

Unlike the 9509 measurement, however, the damage-based method is more conservative than the corresponding maximax results at frequencies between 250 and 1600 Hz. This result is a consequence of two factors, one of which will be inherent in all measurements and the other which may be unique to 9675. For SPLs obtained in higher spectral bands, the maximax result contains more "frequency-smoothing" because, during each overlapping time segment, the narrow-band spectral lines are averaged within each one-third-octave band. Thus, the maximum response at a particular frequency in the spectrum is averaged during each overlapping time segment with other, lower spectral values. Conversely, the damage-based approach passes the flight data through a series of SDOF oscillators spaced at 1/12-octave intervals, retaining the maximum value of the spectral peaks independently. For the damage-based approach, therefore, conversion to one-third-octave SPLs must be performed at the conclusion of data processing. This averaging effect of the maximax method will be inherent in the processing of all measurements.

Unlike the 9509 vibration data, the 9675 data are characterized at higher frequencies by spectral values that appear to be somewhat controlled by transient characteristics. For example, consider the cycle-countplot shown in Fig. 9 for 9675 at 561.2 Hz during mission K-3. The results are shown for Q values of 10, 25, and 50 and are plotted in the format shown in Fig. 4. Notice that the line to A_{max} in Fig. 9 does not fall along the majority of the data points as in Figs. 5 and 6, but, rather, G_1 is controlled by a single cycle for a particular value of Q. This type of result is characteristic of an input excitation containing a transient event. The reasonableness of treating such environments with a single, stationary random test is questionable and it is suggested that, in these cases, the transient be removed and possibly dealt with in a separate test. Nevertheless, note that if the transient is not removed, the derived damage-based spectral values used for the stationary test will still, in an average sense, envelop the maximum flight data response, whereas the test spectral values obtained by using the maximax approach will not.

Conclusions

A damage-based analysis procedure has been described herein that enables the determination of a stationary test spectrum such that both the peak response and the fatigue-damage potential of the nonstationary flight environments are enveloped. The resulting test spectrum is conservative in that it envelops spectra for a range of structural damping and fatigue exponents that encompass the material variability of the hardware. The test criteria that are developed are seen to be much less conservative than the specifications determined by using traditionally employed maximax results. The first important benefit is that, by using the damage-based method to analyze historical data, the predicted overall rms or SPLs for future launch vehicle hardware will, in some cases, be considerably reduced. For equipment that undergo severe flight environments, this reduction in level may be significant enough to avoid the undesirable practice of band splitting during acceptance and qualification testing. The second major benefit of the method is its tendency to provide lower estimates of spectral peak values that have historically been overestimated by the manner in which the maximax approach treats brief periods of strong oscillation in the flight data. It is not uncommon that spectral peak values determined from flight data, acquired on early missions of a new launch vehicle, exceed the specifications to which equipment was originally tested, thus suggesting an inadequate qualification of the hardware. By using the damage-based approach to compare nonstationary flight environments with stationary test criteria, potentially costly requalification programs, driven by the overconservatism inherent in the maximax analysis of flight data, may be avoided. Finally, the damage-based approach does not require measurement-specific determination of optimal signal processing parameters. The potential advantages suggested herein have been demonstrated by analysis of a set of statistically meaningful vibration and acoustic data acquired on the Titan 4A launch vehicle.

Acknowledgments

This work was supported by the U.S. Air Force Space Command, Space and Missile Systems Center, under Contract F04701-00-C-0009. The authors thank Bruce Lowe of Lockheed Martin Astronautics for providing the data used in the analysis, his comments regarding data reduction methods, and his insight into the behavior of the Titan launch vehicle. The authors also acknowledge the data processing support provided by Jessica Jensen of The Aerospace Corporation.

References

[1] Piersol, A. G., "Criteria for the Optimum Selection of Aerospace Component Vibration Test Levels," *Proceedings of the 20th Annual Meeting of the Inst. of Environmental Sciences*, Inst. of Environmental Sciences, Washington, DC, 1974, pp. 88–94.

[2] Piersol, A. G., "The Analysis of Nonstationary Vibration Data," *58th Shock and Vibration Symposium*, Vol. 1, NASA Marshall Space Flight Center, Huntsville, AL, 1987, pp. 3–25.

[3] Himelblau, H., and Piersol, A. G., "Evaluation of a Procedure for the Analysis of Nonstationary Vibroacoustic Data," *Journal of the Institute of Environmental Sciences*, Vol. 32, No. 2, 1989, pp. 35–42.

[4] Piersol, A. G., "Optimum Resolution Bandwidth for Spectral Analysis of Stationary Random Vibration Data," *Journal of Shock and Vibration*, Vol. 1, No. 1, 1993, pp. 33–43.

[5] Piersol, A. G., "Optimum Data Analysis Procedures for Titan 4 and Space Shuttle Payload Acoustic Measurements During Lift-off," NASA CR-190479, Dec. 1991.

[6] Himelblau, H., Kern, D. L., Manning, J. E., Piersol, A. G., and Rubin, S., "Dynamic Environmental Criteria," NASA HDBK-7005, March 2001.

[7] Himelblau, H., Piersol, A. G., Wise, J. H., and Grundvig, M. R., *Handbook for Dynamic Data Acquisition and Analysis*, Inst. of Environmental Sciences, IES-RP-DTE012.1, Mount Prospect, IL, 1995, pp. 287–301.

[8] *Test Requirements for Launch, Upper Stage and Space Vehicles*, Military Standard, MIL-STD-1540C, 15 Sept. 1994.

[9] *Product Verification Requirements for Launch, Upper Stage, and Space Vehicles*, Dept. of Defense Standard Practice, MIL-STD-1540D, 15 Jan. 1999.

[10]*Test Requirements for Launch, Upper Stage, and Space Vehicles, Vol. 1: Baselines*, Dept. of Defense Handbook, MIL-HDBK-340A, 1 April 2001.

[11]*Test Requirements for Launch, Upper Stage, and Space Vehicles, Vol. 2: Applications Guidelines*, Dept. of Defense Handbook, MIL-HDBK-340A, 1 April 2001.

[12]Rubin, S., "Damage-Based Analysis Tool for Flight Vibroacoustic Data," *Proceedings of the 19th Aerospace Testing Seminar*, Inst. of Environmental Sciences Technology, The Aerospace Corp., and Space and Missile Systems Center, 2000.

[13]Lalanne, C., *Mechanical Shock and Vibration, Vol. IV: Fatigue Damage*, 1st ed., Taylor and Francis, Philadelphia, 2002.

[14]Lalanne, C., *Mechanical Shock and Vibration, Vol. V: Specification Development*, 1st ed., Taylor and Francis, Philadelphia, 2002.

[15]Miskel, J. F., III, "Fatigue-Based Random Vibration and Acoustic Test Specification," M.S. Thesis, Dept. of Mechanical Engineering, Massachusetts Inst. of Technology, Cambridge, MA, May 1994.

[16]Bradford, K. B., and Manning, J. E., "Vibroacoustic Intelligent System for Predicting Environments, Reliability, and Specifications (VISPERS)," *Proceedings of the 19th Aerospace Testing Seminar*, 2000, pp. 371–378.

[17]Bendat, J. S., and Piersol, A. G., *Random Data Analysis and Measurement Procedures*, 3rd ed., Wiley, New York, 2000.

[18]Newland, D. E., *An Introduction to Random Vibrations and Spectral Analysis*, 2nd ed., Longman Group, New York, 1984.

[19]Steinberg, D. S., *Vibration Analysis for Electronic Equipment*, 3rd ed., Wiley, New York, 2000, p. 168.

M. P. Nemeth
Associate Editor